ChemComm

Accepted Manuscript

View Article Online
DOI: 10.1039/C8CC03749C

Dual Electrical Switching Permeability of Vesicles via Redox-Responsive Self-Assembly of Amphiphilic Block Copolymers and Polyoxometalates

Dandan Chong, Junyan Tan, Jinlong Zhang, Yue Zhou, Xinhua Wan*, Jie Zhang*

Beijing National Laboratory for Molecular Sciences, Key Laboratory of Polymer Chemistry and Physics of Ministry of Education, College of Chemistry and Molecular Engineering, Peking University, Beijing 100871, P. R. China.

E-mail: xhwan@pku.edu.cn ; jz10@pku.edu.cn

View Article Online
DOI: 10.1039/C8CC03749C

Journal Name

COMMUNICATION

Dual Electrical Switching Permeability of Vesicles via Redox-Responsive Self-Assembly of Amphiphilic Block Copolymers and Polyoxometalates

Received 00th January 20xx,
Accepted 00th January 20xx

DOI: 10.1039/x0xx00000x

www.rsc.org/

Eletro-responsive vesicles were demonstrated based on an amphiphilic block copolymer PEO_{114}-*b*-P(DCH-Ru)$_n$ and an inorganic nanoparticle polyoxometalate $H_3PMo_{12}O_{40}$ (PMo_{12}) via electrostatic interactions. After undergoing electrochemical reactions, vesicle membranes allow the migration of electrolyte ions and release of loaded cargos.

In living organisms, normal cellular activities and functions depend on efficient and selective intra/extracellular communications.[1,2] Under the membrane potentials, permeation and fusion, assembly and disassembly, transmembrane transport of ions and proteins are very typical life phenomena.[3,4] Polymer vesicles[5,6] (known as polymersomes) are good mimic of bilayer membrane owing to their good structural stability, adjustable structural parameters, and flexible functional integration. Their smart performance in response to certain stimuli[7], such as chemical redox, temperature, light, pH, electric potential, are finding increasing applications in drug delivery [8,9], electrical therapy [10,11], and energy storage [12,13]. In particular, development of the electro-responsive polymer vesicles is very significant for simulating and understanding these life activities of cell membranes under the membrane potentials.

The electro-responsive mode can simulate the opening and closing behavior of cell membrane channels under membrane potential control, further to carry out more extensive biomimetic design. Compared with the traditional light and pH stimuli, the voltage is clean and controllable, and leads to smaller cell damage and more convenient implementation. Albeit highly desirable, the electrically off-on switchable and adjustable polymersomes have been far less explored. Yuan [14] reported voltage-responsive reversible assembly and disassembly behaviour of vesicles based on the terminal host-guest interactions between poly(styrene)-β-cyclodextrin and poly(ethylene oxide)-ferrocene. Another vesicular system [15, 16] that is switchable by electric potential was demonstrated using redox-responsive self-assembly of an amphiphilic molecule consisting of a tetraaniline and a poly(ethylene glycol) or poly(*N*-isopropylacrylamide) block. To deeply understand and simulate the transmembrane transport behaviour, an alternative way that does not need to completely dissociate the vesicles, is to simply adjust the membrane walls and permeability of the vesicles.

Beijing National Laboratory for Molecular Sciences, Key Laboratory of Polymer Chemistry and Physics of Ministry of Education, College of Chemistry and Molecular Engineering, Peking University, Beijing 100871, China
E-mail: xhwan@pku.edu.cn; jz10@pku.edu.cn
Electronic Supplementary Information (ESI) available: [details of any supplementary information available should be included here]. See DOI: 10.1039/x0xx00000x

View Article Online
DOI: 10.1039/C8CC03749C

Herein we present a new type of switchable vesicular system with dual electro-responsive mode based on the amphiphilic block copolymer PEO_{114}-*b*-P(DCH-Ru)$_n$ and the inorganic Keggin polyoxometalate PMo_{12} via electrostatic interaction (Figure 1). Electroactive moieties in the inner membrane of supramolecular structure exhibit good electrochemical performance. The coassemblies retain the vesicular structure before and after oxidation or reduction, but the size and permeability change to "breath" in and out of different ions and controlled release of the loaded cargos.

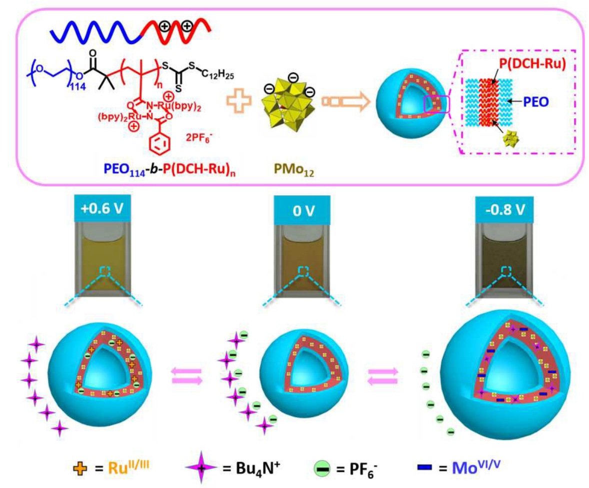

Figure 1. Schematic illustration of the hybrid co-assembly of cationic block copolymer PEO_{114}-*b*-P(DCH-Ru)$_n$ with anionic Keggin polyoxometalate PMo_{12} and transmembrane transport process of different ions.

The block copolymers containing dinuclear ruthenium groups PEO_{114}-*b*-P(DCH-Ru)$_n$ (polyethylene glycol-*b*-poly[benzoic acid *N′*-methylacryloylhydrazide dinuclear ruthenium complex]) were synthesized via combining reversible addition-fragmentation (RAFT) chain transfer polymerization and subsequent ligand-exchange method. Detailed synthetic procedures were described in Supporting Information (Figure S1-S5). A series of diblock copolymer precursors PEO_m-*b*-P(DCH)$_n$ (m and n denote the degree of polymerization of EO and DCH, respectively) were prepared by RAFT polymerization upon varying the feed ratio of the monomer to the PEO_{114}-DMP. ^{1}H NMR measurements further confirm the chemical structures and compositions of PEO_m-*b*-P(DCH)$_n$ (m = 114; n = 4, 10, 14). The copolymers PEO_m-*b*-P(DCH)$_n$ have monodispersities of 1.2-1.3 indicated by GPC in DMF/0.1 M LiBr as an eluent. The corresponding complex copolymers PEO_m-*b*-P(DCH-Ru)$_n$ were synthesized through the ligand-exchange method with *cis*-$Ru(bpy)_2Cl_2 \cdot H_2O$ (bpy = 2,2'-bipyridine) according to the procedure described previously [17,18]. The complex ratio of Ru in diblock copolymers determined by ICP analysis is about 50%. These characteristic data were summarized in Table S1.

The PEO_{114}-*b*-P(DCH-Ru)$_n$/PMo_{12} coassemblies were prepared by the addition of PMo_{12} solution to a dilute PEO_{114}-*b*-P(DCH-Ru)$_n$ solution in CH_3CN at the charge ratio ~1:1 based on the electrostatic interaction between the cationic copolymers PEO_{114}-*b*-P(DCH-Ru)$_n$ and the anionic polyoxometalates PMo_{12}. Both the dinuclear ruthenium compounds [19] and polyoxometalates [20, 21 22] are electrochromic in the wide UV-vis-NIR region, and their individual electrochemical activities are expected to be maintained in the thus-prepared coassemblies. The UV-vis-NIR spectroelectrochemistry method was used to track the characteristic absorption bands of redox species at different electrochemical state of these hybrid coassemblies (Figure 2). In the presence of electrolytes, the original state of the coassemblies were at the Ru^{II}/Ru^{II} and Mo^{VI}/Mo^{VI} state. By applying the +0.6 V potential, the absorption bands are typically at about 1600 nm assigned to the intramolecular inter-valence charge transfer (IVCT) transitions of the Ru^{II}/Ru^{III} species. Under the applied potential of -0.8 V, the absorption bands are broad covering the visible and near-infrared region of 700~1200 nm and assigned to the IVCT transitions of the Mo^{VI}/Mo^{V} species.

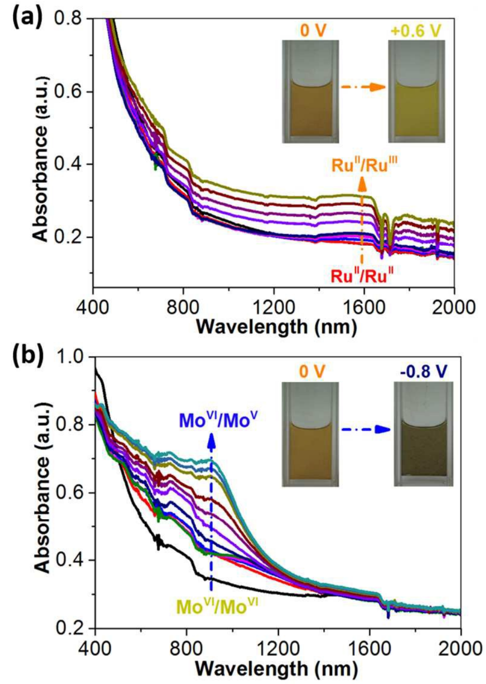

Figure 2. UV-vis-NIR absorption spectra and electrochromism of the coassemblies of PEO_{114}-*b*-P(DCH-Ru)$_{14}$/PMo_{12} in CH_3CN with 0.1 M Bu_4NPF_6 .

To identify the structures of coassemblies formed by cationic PEO_{114}-*b*-P(DCH-Ru)$_n$ with anionic PMo_{12}, we observed the samples oxidized or reduced at various voltages by using different microscopes. The statistical data were shown in Table S1. For PEO_{114}-*b*-P(DCH-Ru)$_n$/PMo_{12} (n = 10, 14) coassemblies, TEM images, SEM images, and AFM images showed vesicular structures (Figure S6, Figure 3 and S7). Taking PEO_{114}-*b*-P(DCH-Ru)$_{14}$/PMo_{12} as an example, the initial average diameter of vesicles at 0 V state was about 103 ± 12 nm (Figure 3a). As we

View Article Online
DOI: 10.1039/C8CC03749C

know, when the two partially fused vesicles diffused into separate ones, an open-mouth-like pole [23] and different types of intermediates could be formed. The height ~20 nm in AFM was much smaller than the horizontal size ~100 nm, further indicating the vesicular structures. When the positive voltage +0.6 V was applied, the vesicle size expanded to be 245 ± 26 nm (Figure 3b). A part of ruptured vesicles with the wall thickness ~40 nm in TEM and the open-mouth vesicles in SEM clearly confirmed the bilayer membrane structures. When the negative voltage -0.8 V was applied, the vesicle size increased significantly to about 332 ± 40 nm (Figure 3c). Furthermore, the low height to diameter ratio 0.2-0.3 calculated from AFM indicated hollow structure of the vesicles. More TEM images of the ruptured vesicles and intermediates were shown in Figure S8, and clearly confirmed the hollow structure of the vesicles. Besides, the elemental maps of Mo and Ru revealed that the PMo_{12} and DCH-Ru moieties were dispersed on the vesicle (Figure S9). These results proved the hybrid assemblies in a bilayer pattern at the membrane interface for PEO_{114}-*b*-P(DCH-Ru)$_n$/PMo_{12} (n = 10, 14). The amphiphilic block copolymer PEO_{114}-*b*-P(DCH-Ru)$_4$ with shorter dinuclear ruthenium chain can form spherical micelles when self-assembling with PMo_{12} (Figure S10). All the hybrid coassemblies PEO_{114}-*b*-P(DCH-Ru)$_n$/PMo_{12} (n = 4, 10, 14) can be adjusted by corresponding oxidation or reduction potentials.

To further identify the chemical composition and content variation before and after electrochemical stimulus, we measured the X-ray photoelectron spectroscopy (XPS) of the coassemblies. The contents of Ru, N, P, Mo, and other representative elements in the coassemblies determined by the observed signal peaks in the full spectrum proved the structural integrity in the self-assembly structures (Figure S11 and Table 1). At +0.6 V state, the coassemblies showed the content of F increased by 6.58% and the content of N decreased by 0.83% with Mo decreased by 0.21% compared with those at the 0 V state, indicating that PF_6^- came in and Bu_4N^+ went out of the expansive vesicles. At -0.8 V state, the system showed the content of N increased by 3.51% with Mo increased by 1.75% and the content of F decreased by 4.56% compared with those at the 0 V state, indicating that Bu_4N^+ came in and PF_6^- went out of the expansive vesicles. Both in positive and negative electrochemical stimuli, the variation trend of Mo contents indicated the PMo_{12}^-/Bu_4N^+ symport and PMo_{12}^-/PF_6^- antiport.

Based on the redox states in the spectroelectrochemical tests and the assembling structures, we proposed charge-compensation mechanism to explain transmembrane transport process (Figure 1). In the case of vesicles, PEO acted as the stabilizing part in the core and shell of vesicles, and the skeleton membrane structures were the P(DCH-Ru)/PMo_{12} part. At the original state, the coassemblies were at Ru^{II}/Ru^{II} and Mo^{VI}/Mo^{VI} state and some small ions such as Bu_4N^+ and PF_6^- existed in the electrolyte solution. When the oxidation potential +0.6 V was applied, the Ru^{II}/Ru^{II} component was oxidized to the mixed-valence state Ru^{II}/Ru^{III}; and thus the internal P(DCH-Ru)/PMo_{12} complex became excessively positively charged and mutually repulsed, so that the vesicle expanded and the size increased to allow the negative ions PF_6^- into the system for charge compensation. The positive ions Bu_4N^+ were excluded out from the membrane in company with the counterions PMo_{12}^{3-}. When the reduction potential -0.8 V was applied, the Mo^{VI}/Mo^{VI} component was reduced to the mixed-valence state Mo^{VI}/Mo^{V}; the local excessive negative charges excluded out of other anions PF_6^-, and the vesicles expanded with the entrance of cations Bu_4N^+ for charge compensation. Meanwhile, the reductive polyoxometalate nanoparticles $PMo_{12}^{4-/5-}$ with higher charges easily entered into the overinflated vesicles. The above-mentioned transmembrane transport process of different ions were consistent with the XPS results. This phenomenon mimicking the voltage-gated ion channels and selective intra/extracellular communications in cell bilayer membranes, may help understand these life activities of living organisms.

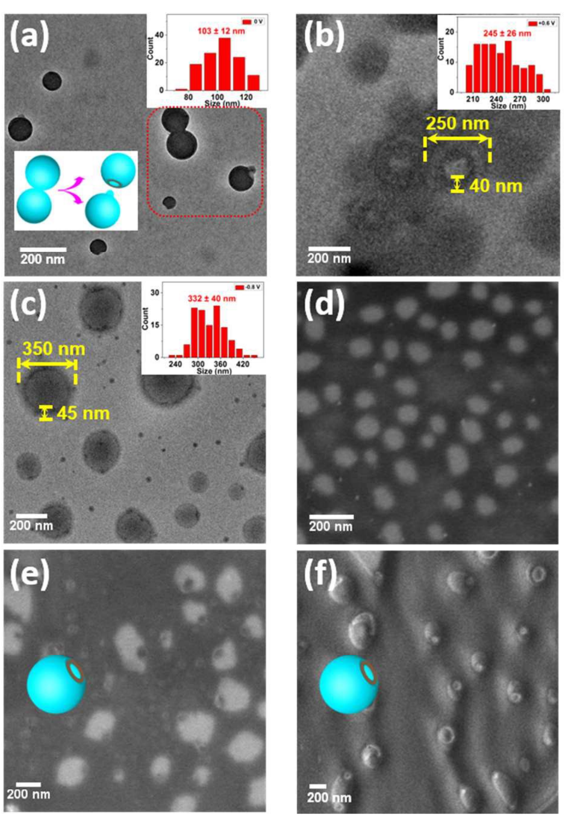

Figure 3. TEM images at (a) 0 V, (b) +0.6 V, (c) -0.8 V; SEM images at (d) 0 V, (e) +0.6 V, (f) -0.8 V state of the hybrid coassemblies PEO_{114}-*b*-P(DCH-Ru)$_{14}$/PMo_{12}.

Table 1. Content analysis of characteristic elements in XPS full spectra of PEO_{114}-*b*-P(DCH-Ru)$_{14}$/PMo_{12} at different state.

	0 V	+0.6 V [a]	Δ (%)	Ion	-0.8 V [a]	Δ (%)	Ion
C	74.02	74.06	0.04	/	73.96	-0.06	/
N	6.26	5.43	-0.83	Bu_4N^+ (out)	9.77	3.51	Bu_4N^+ (in)
F	10.12	16.70	6.58	PF_6^- (in)	5.56	-4.56	PF_6^- (out)
P	2.88	4.74	1.86	/	2.40	-0.48	/
Mo	0.8	0.59	-0.21	PMo_{12}^- (out)	2.55	1.75	PMo_{12}^- (in)
Ru	5.92	5.92	0.00	/	5.92	0.00	/

[a] The large copolymer structures constitute the stable framework of vesicles, so the content of Ru was normalized in order to estimate the content variation of other small ions.

View Article Online
DOI: 10.1039/C8CC03749C

By using the feature of voltage response, these vesicles can be used for drug loading and controlled release, as a simple biomimetic model to simulate expansion movement of the bilayer membrane of biological cells through membrane potential to release the target molecules. In order to study the potential application of the vesicles in controlled release system, we used fluorescent Rhodamine B (RhB) as a model drug molecule. The release process was carried out under positive oxidation potentials. As shown in Figure 4, when the +0.6 V voltage was applied, the vesicle was inflated, then the internal loaded fluorescent dye RhB could be released from the vesicles, and the fluorescence intensity reached maximum within 3 hours. In the control experiment without any stimuli, the early increase was in accordance with the free release model, and the later decline was due to the gradual photobleaching effect of organic dye molecules. The traditional drug-delivery systems, generally realized at the acidic pH value or the addition of redox reagents to stimulate the release process, might introduce additional interference or pollution to the system. In comparison, the voltage stimulation mode in the above electro-responsive systems is relatively clean and controllable.

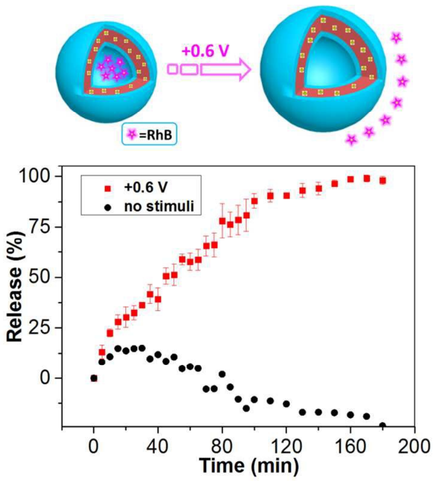

Figure 4. Controlled release of RhB from the supramolecular vesicles PEO_{114}-*b*-P(DCH-Ru)$_{14}$/PMo_{12} under oxidation potential stimuli and in comparison with the free release of RhB from the vesicles without stimuli.

In summary, dual electro-responsive vesicles, based on hybrid electrostatic assemblies of a series of amphiphilic block copolymers PEO_{114}-*b*-P(DCH-Ru)$_n$ and the inorganic nanocluster polyoxometalate PMo_{12}, were demonstrated, regulating by corresponding oxidation or reduction potentials. Furthermore, accompanied by electrochemical reactions, vesicle membranes necessitate the migration of supporting electrolyte ions and the controlled release of loaded target molecules. From the point view of stimulating sources, a new dual-voltage response mode was developed to simulate and understand cell life activities through cell membrane potentials. From the perspective of functionalities, the supramolecular assembly can promote photoelectric properties, expanding the application in tailorable optoelectronic materials.

This work was supported by the National Natural Science Foundation of China (grant numbers 51673002 and 21322404). We would like to thank Anchao Feng and Prof. Jinying Yuan at Tsinghua University for helpful discussions in the controlled release experiments.

Notes and references

1. M. J. York-Duran, M. Godoy-Gallardo, C. Labay, A. J. Urquhart, T. L. Andresen and L. Hosta-Rigau, *Colloid Surfaces B*, 2017, **152**, 199-213.
2. R. H. Fang, Y. Jiang, J. C. Fang and L. F. Zhang, *Biomaterials*, 2017, **128**, 69-83.
3. S. Chen, Y. Zhao, C. Bao, Y. Zhou, C. Wang, Q. Lin and L. Zhu, *Chem. Commun.*, 2018, **54**, 1249-1252.
4. X. Bao, X. Wu, S. N. Berry, E. N. W. Howe, Y.-T. Chang and P. A. Gale, *Chem. Commun.*, 2018, **54**, 1363-1366.
5. J. Z. Du and R. K. O'Reilly, *Soft Matter*, 2009, **5**, 3544-3561.
6. J. Gaitzsch, X. Huang and B. Voit, *Chem. Rev.*, 2016, **116**, 1053-1093.
7. X. L. Hu, Y. G. Zhang, Z. G. Xie, X. B. Jing, A. Bellotti and Z. Gu, *Biomacromolecules*, 2017, **18**, 649-673.
8. M. Huo, J. Yuan, L. Tao and Y. Wei, *Polym. Chem.*, 2014, **5**, 1519-1528.
9. Y. Zhao, A. C. Tavares and M. A. Gauthier, *J. Mater. Chem. B*, 2016, **4**, 3019-3030.
10. N. Casado, G. Hernandez, H. Sardon and D. Mecerreyes, *Prog. Polym. Sci.*, 2016, **52**, 107-135.
11. C. Xie, P. Li, L. Han, Z. Wang, T. Zhou, W. Deng, K. Wang and X. Lu, *Npg Asia Mater.*, 2017, **9**, e358.
12. R. Gracia and D. Mecerreyes, *Polym. Chem.*, 2013, **4**, 2206-2214.
13. M. Burgess, J. S. Moore and J. Rodriguez-Lopez, *Acc. Chem. Res.*, 2016, **49**, 2649-2657.
14. Q. Yan, J. Yuan, Z. Cai, Y. Xin, Y. Kang and Y. Yin, *J. Am.Chem. Soc.*, 2010, **132**, 9268-9270.
15. H. Kim, S.-M. Jeong and J.-W. Park, *J. Am.Chem. Soc.*, 2011, **133**, 5206-5209.
16. Y. Wu, S. Liu, Y. Tao, C. Ma, Y. Zhang, J. Xu and Y. Wei, *ACS Appl. Mater. Interfaces*, 2014, **6**, 1470-1480.
17. W. R. Lin, Y. J. Zheng, J. Zhang and X. H. Wan, *Macromolecules*, 2011, **44**, 5146-5154.
18. D. D. Chong, X. H. Wan and J. Zhang, *J. Mater. Chem. C*, 2017, **5**, 6442-6449.
19. S. Wang, X. Z. Li, S. D. Xun, X. H. Wan and Z. Y. Wang, *Macromolecules*, 2006, **39**, 7502-7507.
20. T. Yamase, *Chem. Rev.*, 1998, **98**, 307-325.
21. H. R. Sun, S. Y. Zhang, J. Q. Xu, G. Y. Yang and T. S. Shi, *J. Electroanal. Chem.*, 1998, **455**, 57-68.
22. H. X. Gu, L. H. Bi, Y. Fu, N. Wang, S. Q. Liu and Z. Y. Tang, *Chem. Sci.*, 2013, **4**, 4371-4377.
23. Q. Geng, J. Xiao, B. Yang, T. Wang and J. Du, *ACS Macro Lett.*, 2015, **4**, 511-515.

View Article Online
DOI: 10.1039/C8CC03749C

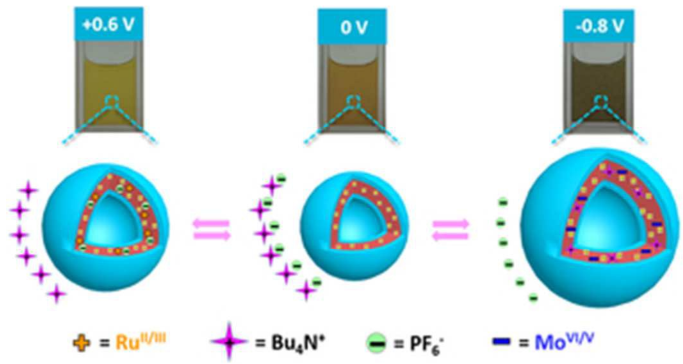

28x15mm (300 x 300 DPI)